Search for Gamow-Teller strength in the continuum via the ^{3}He$(n,p)^3$H reaction at 288 MeV

A. Celler,[1] S. Yen,[2] W. P. Alford,[1] R. Abegg,[2] B. A. Brown,[3] S. Burzynski,[4,*] D. Frekers,[2] O. Häusser,[2,4] R. Helmer,[1,2] R. S. Henderson,[5] K. Hicks,[6] K. P. Jackson,[2] R. Jeppesen,[4] C. A. Miller,[2] M. A. Moinester,[7] B. W. Pointon,[4] A. Trudel,[4] and M. C. Vetterli[2,4]

[1]*University of Western Ontario, London, Ontario, Canada N6A 3K7*

[2]*TRIUMF, 4004 Wesbrook Mall, Vancouver, British Columbia, Canada V6T 2A3*

[3]*Department of Physics and Astronomy, Michigan State University, East Lansing, Michigan 48824*

[4]*Simon Fraser University, Burnaby, British Columbia, Canada V5A 1S6*

[5]*University of Melbourne, Parkville, Victoria, Australia 3052*

[6]*Ohio University, Athens, Ohio 45701*

[7]*Tel-Aviv University, 69978 Ramat Aviv, Israel*

(Received 8 September 1992)

Cross sections for the ^{3}He(n,p) reaction were measured at angles of 2.7°, 7.5°, 14.4°, 28.2°, and 34.9° (c.m.) at an incident beam energy of 288 MeV. Outgoing protons were observed to energies corresponding to a Q value of -40 MeV. The reduced cross section for the Gamow-Teller component of the ground-state isobaric-analog transition was determined to be $\hat{\sigma}=\sigma(q=0)/B_{GT}=6.9\pm0.2$ mb/sr. This value is significantly smaller than that observed for nuclei in the mass range $6\leq A\leq 13$. A multipole analysis of the data indicates that the cross section of the continuum up to a Q value of -20 MeV involves mainly $\Delta L=1$ spin dipole transitions. The analysis determines an upper limit of 0.06 units of Gamow-Teller strength in transitions to excited states between 7 and 16 MeV, but is consistent with no Gamow-Teller strength in this region. Distorted wave impulse approximation calculations using transition amplitudes from a large-scale shell model calculation provide a good fit to the measured ground-state cross section, but fail to account for the magnitude of the measured cross sections to the continuum below 30 MeV excitation.

PACS number(s): 24.50.+g, 25.40.−h, 25.40.Kv, 27.10.+h

I. INTRODUCTION

There has been extensive interest in the problem of the missing strength in Gamow-Teller (GT) beta decay and in the analogous process of (p,n) or (n,p) charge exchange reactions. Theoretical studies have indicated that several different effects are involved in decreasing the expected total strength, with configuration mixing accounting for a substantial fraction of the total loss [1,2]. If this conclusion is correct, then the strength missing at low excitation energies should appear at higher excitation. Although a number of experiments have attempted to identify this expected GT strength at high excitations, results have been inconclusive, mainly because of the difficulty of identifying small amounts of GT strength superimposed on transitions of higher multipolarity. The problem becomes increasingly serious as excitation energy increases because of the decrease in the magnitude of the $\sigma\tau$ effective interaction with increasing momentum transfer, at the same time as the tensor interaction becomes dominant.

The ^{3}He$(n,p)^3$H reaction provides a particularly favorable case in which to search for missing GT strength. Careful measurements of B_{GT}, the square of the GT matrix element, in the ^{3}H$\rightarrow{}^3$He beta decay are available [3], and detailed model calculations [4] show good agreement with measurements. The determination of the cross section for the ground-state transition in the ^{3}He$(n,p)^3$H reaction then yields a measurement of the reduced cross section [5] $\hat{\sigma}=\sigma(q=0)/B_{GT}$ for $A=3$. This result provides a firm basis for estimating the cross section for predicted excited-state transitions associated with the missing GT strength.

A further advantage arises from the fact that the low-lying excitations in $A=3$ are expected to be relatively simple, arising mainly (in a shell model picture) from $0s\rightarrow 0p$ single-particle transitions. Such states will be populated in reactions with angular momentum transfers with $\Delta L=1$, and distorted wave impulse approximation (DWIA) calculations predict that, as a result of relatively small distortion effects for $A=3$, the forward angle cross sections for such transfers are small relative to $\Delta L=0$, even at excitation energies of 20 MeV. Thus the possibility of detecting small GT contributions to the cross section should be more favorable than in heavier nuclei.

II. EXPERIMENTAL MEASUREMENTS

Measurements were carried out using the TRIUMF charge-exchange facility operating in the (n,p) mode. The system is described in detail in Ref. [6]. In the present experiment, neutrons were produced by an achromatic proton beam of energy 290 MeV and intensity 250 nA focused on a ^{7}Li target 220 mg/cm^2 in thickness. The resulting neutron flux on the ^{3}He target was about 10^5/s cm^2.

The ^{3}He gas was contained in a high-pressure gas target, described in Ref. [7]. The single target cell 6.5×3

*On leave from Institute for Nuclear Studies, Swierk, Poland.

cm^2, 9 cm in length, contained 2 l(STP) of ^3He at a pressure of about 2 MPa (20 atm), to give a target thickness of 26 mg/cm^2 of ^3He. The chamber also contained a target of CH_2 of thickness 44.5 mg/cm^2, mounted behind the gas cell, which served to measure the neutron flux on the ^3He target cell.

Protons from the (n,p) reaction on both targets were analyzed by the TRIUMF medium-resolution spectrometer (MRS). Proton spectra were recorded at MRS laboratory angles of 0°, 5°, 10°, 20°, and 25°. Because of the finite angular acceptance of the MRS, data were recorded over a range of about ±2° at each angle setting. The corresponding values of the mean scattering angles, determined experimentally using the ray-tracing capabilities of the MRS, were 2.7°, 7.5°, 14.4°, 28.2°, and 34.9° in the center-of-mass system.

Corrections to the experimental data are required for several effects: (i) background from the counter gas and other counter components in the gas cell, (ii) variation in the MRS acceptance as a function of proton energy, (iii) variations in the neutron flux between the ^3He cell and the CH_2 target, and (iv) the effect of the continuum in the incident neutron spectrum from the $^7Li(p,n)$ reaction.

Data required for the first three of these corrections were obtained by auxiliary measurements at each MRS angle in which the ^3He in the target cell was replaced by either the standard counter gas (90:10 Ar:CO_2) for the first effect or CH_4 for the second and third. The continuum in the incident neutron spectrum was obtained by subtracting a suitably normalized spectrum from the $^{12}C(n,p)$ reaction from a spectrum from a CH_2 target at a MRS angle of 0°. A more detailed discussion of the corrections is given in Refs. [8] and [9], which describe the use of the gas target in studies of the $^{20}Ne(n,p)^{20}F$ and $^{15}N(n,p)^{15}C$ reactions.

III. DATA ANALYSIS AND RESULTS

The raw spectrum at a MRS angle of 0° is shown in Fig. 1, along with the corresponding background spectra from counter gas and from other counter components (solids spectrum). Figure 2 shows the spectrum after background subtraction and after deconvolution of the effect of the continuum in the incident neutron spectrum. This deconvolution does not affect the peak from the isobaric-analog ground-state transition, but clearly is important for the continuum part of the $^3He(n,p)$ spectrum. The energy resolution was about 1.4 MeV at 0°, with an increase to 3 MeV at 25° as a result of multiple scattering in the stainless steel exit window of the target box.

The magnitude of the cross section for the $^3He(n,p)^3H$ reaction was determined by comparing the counting rate for the ground-state transition from the ^3He target with that from the $^1H(n,p)n$ reaction in the CH_2 reference target. After correction for the effects noted above, the ratio of cross sections at a mean laboratory angle of 1.9° (MRS angle 0°) was $\sigma(^3He)/\sigma(^1H)|_{1.9°}=0.738$. The cross section for the $^1H(n,p)$ reaction was not measured directly, but was determined to be $\sigma(^1H,\ 1.9°$ laboratory$)=50.55$ mb/sr using the program SAID [10] with SM 90 phase shifts.

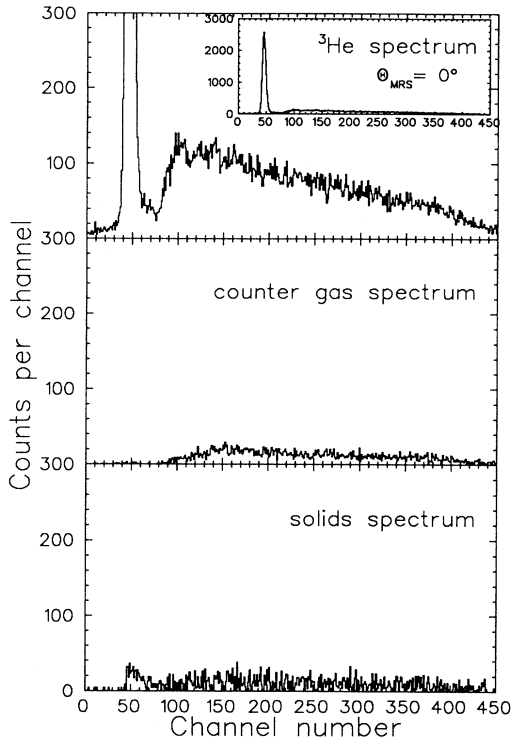

FIG. 1. Raw spectra measured at a MRS angle of 0°. The top panel is the $^3He(n,p)^3H$ spectrum including background. The center panel shows the background contribution from counter gases and the bottom panel the background from structural components of the target cell. All spectra are normalized to the same incident neutron flux.

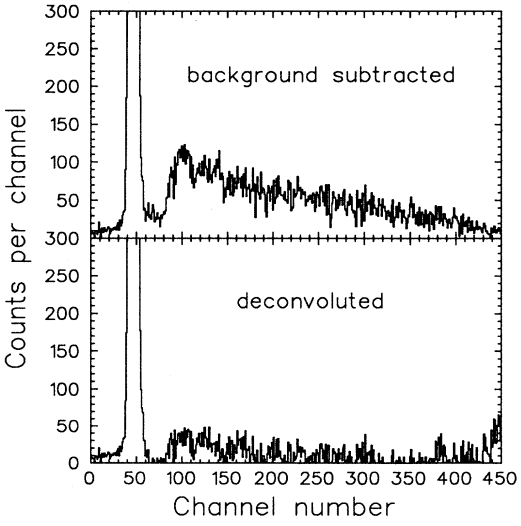

FIG. 2. Upper panel: proton spectrum from $^3He(n,p)^3H$ at a MRS angle of 0° after subtraction of background contributions shown in Fig. 1. Lower panel: final spectrum after correction for MRS acceptance and deconvolution of contributions from continuum in the incident neutron beam. The increase near channel 450 arises from uncertainties in the acceptance correction.

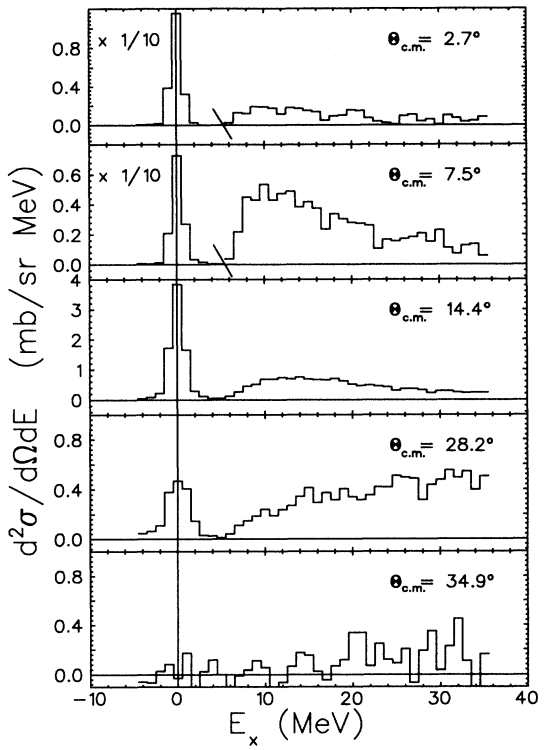

FIG. 3. Final experimental spectra at mean c.m. angles of 2.7°, 7.5°, 14.4°, 28.2°, and 34.9°. The data have been summed in bins of 1 MeV width.

The final spectra with all corrections are shown in Fig. 3 for each angle. In these spectra the data have been summed in bins of width 1 MeV to reduce statistical fluctuations. The uncertainty in the final cross sections arises from several sources: (i) statistical uncertainties in the raw spectra which ranged from 1% for the ground-state transition at 0° to 40% for some of the data at 25°; (ii) statistical uncertainties in the ^{1}H(n,p) reference spectra, which ranged from <1% at 0° to 15% at 25°; (iii) uncertainties in background subtraction, which were generally less than 1%; (iv) uncertainty in the correction for spectrometer acceptance was less than 1%; (v) the uncertainty in the correction for angular variation in neutron flux at large angles was estimated to be less than 5%; and (vi) uncertainty in the deconvolution of the neutron continuum is set by statistical uncertainty in the ^{7}Li(p,n) source spectrum and is expected to contribute less than 5% to the uncertainty in the final data for transitions to excited states.

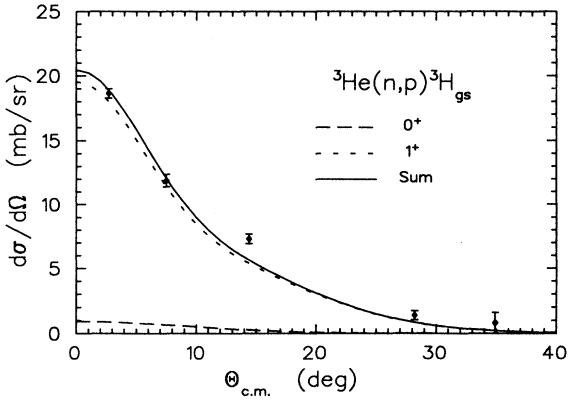

FIG. 4. Comparison of the angular distribution of the ^{3}He(n,p)^{3}H ground-state transition with results of DWIA calculations using the full shell model transition amplitude. The DWIA result has been renormalized by a factor of 0.85. The separate contributions of both the Fermi ($\Delta J^\pi = 0^+$) and Gamow-Teller ($\Delta J^\pi = 1^+$) cross sections are shown, along with their sum.

The angular distribution for the transition to the ^{3}H ground state is shown in Fig. 4 along with the results of DWIA calculations to be discussed later.

IV. MODEL CALCULATIONS AND DATA COMPARISON

A. Shell model

In the simplest model, the ground states of the $A=3$ nuclei ^{3}He and ^{3}H are described by three nucleons in the $0s_{1/2}$ shell. There is clear evidence, however, that such a simple model is inadequate. For instance, the beta decay rate of tritium [3] is about 8% less than predicted by this model. Less directly, it has been shown that calculations of the binding energy of ^{4}He require inclusion of excitations up to $10\hbar\omega$ in order to reproduce the measured binding [11], and comparable excitations would be expected in $A=3$ nuclei as well. It has also been shown [12] that in Faddeev calculations of the binding energy of ^{3}H up to 34 channels are required in order to achieve convergence.

Using the shell model code OXBASH [13], we have carried out calculations which include $0\hbar\omega$ plus $2\hbar\omega$ excitations for even-parity states and $1\hbar\omega$ plus $3\hbar\omega$ for odd-parity states. Calculations were done in an oscillator basis with oscillator energy $\hbar\omega = 10$ MeV, and an effective interaction taken from Hosaka, Kubo, and Toki [14]. This interaction was developed to remedy some recognized shortcomings of other effective interactions such as M3Y [15]. It was shown to be independent of nuclear mass for $16 \le A \le 90$, so that our use of it for $A=3$ is not unreasonable. The calculation predicts a rms charge radius of 2.0 fm for the ground state, in reasonable agreement with the measured value of 1.88 fm [16]. The strength of the GT component in the ground-state beta decay of tritium is calculated as $B_{GT}=2.85$, compared with the experimental value [3] of $B_{GT}=2.77$.

Wave functions were calculated for all states in the model space, which extended to an excitation energy of about 50 MeV. This included states of spins $\frac{1}{2} \le J \le \frac{9}{2}$ with both positive and negative parity. These were then used to calculate single-particle transition amplitudes for all final states in the ^{3}He(n,p)^{3}H reaction.

B. DWIA

Calculations of cross sections for the ^{3}He(n,p)^{3}H reaction were carried out using the code DW81 [17]. Optical potentials required for the calculations were taken from a study of the ^{4}He(p,$2p$) reaction at intermediate energies [18]. In that work, optical parameters were derived by fitting elastic scattering data for $p+^3$He and $p+^3$H at in-

TABLE I. Optical model potentials with $V=V_{\rm Coul}+Vf(r,R_R,a_R)+iWf(r,R_I,a_I)-(V_{\rm s.o.}+iW_{\rm s.o.})g(r,R_{\rm s.o.},a_{\rm s.o})(\mathbf{s}\cdot\mathbf{l})$, $f(r,R_i a_i)=\{1+\exp[(r-R_i)/a_i]\}^{-1}$, and $g(r,R_i a_i)=-\frac{2}{r}[\hbar/m_\pi c]^2(d/dr)[f(r,R_i,a_i)]$. Potentials in MeV, radii in fermi.

	V	R_R	a_R	W	R_I	a_I	$V_{\rm s.o}$	$W_{\rm s.o}$	$R_{\rm s.o.}$	$a_{\rm s.o.}$	$r_{\rm Coul}$
$n+{}^3$He	−11.39	1.443	0.083	−12.93	1.636	0.247	7.14	15.76	0.950	0.260	1.3
$p+{}^3$H	−13.85	1.440	0.194	−10.13	1.770	0.247	13.58	−1.20	1.050	0.280	1.3

termediate energies. In the present work, optical parameters for the $(n+{}^3\text{He})$ entrance channel were obtained by interpolation from the $(p+{}^3\text{He})$ parameters at 156 and 415 MeV, while those for the $(p+{}^3\text{H})$ exit channel were obtained by interpolation from the $(p+{}^3\text{H})$ parameters at the same energies. These parameters are shown in Table I. To test the sensitivity of the results to the choice of optical potentials, calculations were also carried out using either the $(p+{}^3\text{He})$ or $(p+{}^3\text{H})$ parameters in both entrance and exit channels. For GT transitions the angular distributions showed no significant change, while the zero-degree cross section was constant to within about 2%. Calculations with the energy-dependent average parameters given in Ref. [18] also showed no significant change in the shape of the angular distributions, although the zero-degree cross sections for GT transitions varied over a range of about 20% relative to those calculated with the interpolated parameters. For transitions with $\Delta L>0$, the behavior was similar. The shapes of the calculated angular distributions showed very little dependence on the choice of optical potentials, while peak cross sections showed variations in magnitude comparable to those for GT transitions.

Single-particle states were described by harmonic oscillator wave functions with oscillator parameter $b=1.4$ fm for the ground states of ^{3}He and ^{3}H. This choice of b yields a rms radius for a bound proton in good agreement with the point proton radius deduced [19] from electron scattering on ^{3}He. For unbound excited states in the final nucleus, the effect of the expected spatial spreading of the wave function was approximated by increasing the magnitude of the oscillator parameter b. As this was increased to a value $b_{\rm final}=2$ fm, the peak cross section for 1^- transitions decreased in magnitude by 40%, while the location of the peak shifted to smaller angles, as expected. For still larger values of b, the shapes showed little further change, but decreased in magnitude as the overlap between initial and final single-particle states decreased. A value of $b_{\rm final}=2$ fm was used in the final calculations.

The effective interaction used in the calculations was the Franey-Love interaction [20] for $E=270$ MeV. Using the shell model transition amplitudes described earlier, DWIA cross sections were calculated for all transitions up to an excitation energy of 30 MeV, for comparison with measured spectra.

C. Data comparison

1. Ground state

The calculated angular distribution for the ground-state transition is compared with the data in Fig. 4. Both the GT and Fermi interactions can contribute to this transition, and the calculated cross section for each component, as well as their sum, is shown in Fig. 4. The magnitudes of each calculated cross section have been renormalized by a factor of 0.846 in order to fit the measured cross section. A renormalization of this magnitude is within the range expected for different choices of optical potentials and is not considered significant here.

The results for the ground-state transition were also used to estimate the reduced cross section $\hat{\sigma}=\sigma_{\rm GT}(q=0)/B_{\rm GT}$ for mass $A=3$. For this determination the measured cross section at a laboratory angle of 1.9° (2.7° c.m.) was extrapolated to a cross section for $q=0$ at 0° using DWIA calculations with the same parameters as used in fitting the angular distribution. The contribution to this extrapolated cross section from the Fermi interaction was obtained from the DWIA calculation as $\sigma_F(q=0)=0.9$ mb/sr. This then yielded the estimate $\sigma_{\rm GT}(q=0)=19.3\pm0.4$ mb/sr. The quoted uncertainty is an estimate of the effect of counting statistics, DWIA extrapolation, and various experimental corrections listed earlier. With the value $B_{\rm GT}=2.77$ taken from Ref. [3], we obtain a value $\hat{\sigma}=6.93\pm0.15$ mb/sr.

In addition to the experimental uncertainties noted, there is a systematic uncertainty of about 2% in the absolute magnitude of the cross section arising from uncertainties in the phase shifts used in SAID [10]. As a final value, we therefore concluded

$$\hat{\sigma}=6.9\pm0.2 \text{ mb/sr} .$$

2. Excited states

The only bound states in $A=3$ nuclei are the ground states of ^{3}He and ^{3}H, so that aside from the ground-state peak the cross sections shown in Fig. 3 represent transitions to the continuum. The shell model calculations predict the first excited state $(\frac{1}{2}^-, T=\frac{1}{2})$ at 10.4 MeV, well above the neutron separation energy of 6.26 MeV for ^{3}H. Consequently, in making a comparison between the shell model predictions and the measured spectra, the DWIA cross section for each predicted state was assumed to be spread with a Gaussian distribution of a full width at half maximum (FWHM) of 5 MeV. A calculated reaction cross section as a function of excitation energy was then constructed by summing contributions from all predicted states up to 30 MeV.

The comparison with the measured cross sections is shown in Fig. 5. At 2.7° the predicted peak near 12 MeV excitation contains about equal contributions from 1^+ $(\Delta L=0)$ and 1^- $(\Delta L=1)$ contributions, while the predicted cross section is equal to about two-thirds of the

measured magnitude. At higher excitation a second peak is predicted near 24 MeV, with about half the cross section arising from an isovector monopole ($\Delta L=0$) transition to the lowest $\frac{1}{2}^+$ $T=\frac{3}{2}$ state and about one-third arising from several $\Delta L=1$ transitions to negative-parity states in this energy region. Agreement with the data is poor, with the measured cross section between 20 and 30 MeV about an order of magnitude smaller than the model predictions.

At 14°, which is near the maximum of the calculated cross sections for $\Delta L=1$ transitions, the predicted peak near 12 MeV excitation arises almost entirely from $\Delta L=1$ transitions. The magnitude of the peak is only about one-quarter of the measured cross section, however. Thus it is seen that overall agreement between the data and model predictions is poor, in marked contrast to results obtained in the study [9] of the ^{15}N(n,p) reaction. This represents a serious failure of the calculations, but the reasons for the disagreement are not clear.

We note that agreement between data and calculations is good for the ground-state transition. In this case the wave functions are known to be satisfactory since they predict the GT transition strength B_{GT}, in good agreement with that measured in the beta decay of tritium.

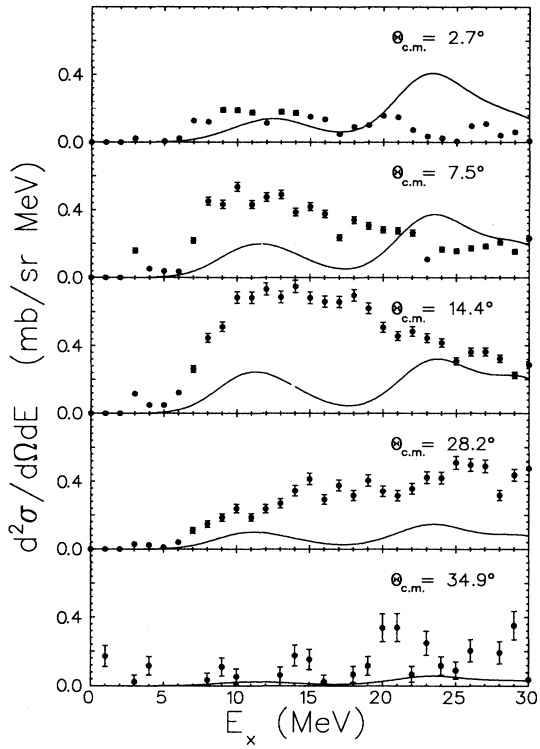

FIG. 5. DWIA cross sections for transitions to excited states calculated using full shell model transition amplitudes. The contribution from each model state has been spread over a Gaussian distribution of 5 MeV (FWHM). For comparison, the measured cross sections to the continuum are also shown. These are the same as in Fig. 3 with cross section for the ground-state transition ($E_x \leq 2$ MeV) set equal to zero at all angles except 34.9°.

Thus the agreement with the DWIA calculations indicates that the reaction model is satisfactory.

For transitions to excited states, it is unlikely that the disagreement between data and calculations reflects a failure of the shell model wave functions. Low-lying states of negative parity are expected to arise mainly from the $1\hbar\omega$ transitions $0s_{1/2}\rightarrow 0p_{1/2}$ and $0s_{1/2}\rightarrow 0p_{3/2}$, and the model calculations show these as the most important components in transition amplitudes for excited states below 15 MeV excitation. DWIA calculations were carried out for pure $0s\rightarrow 0p$ transitions to states at an assumed excitation energy of 10 MeV with the result that predicted cross sections at 14° were 0.7 mb/sr for $s_{1/2}\rightarrow p_{1/2}$ and 1.5 mb/sr for $s_{1/2}\rightarrow p_{3/2}$. In comparison, the full shell model wave functions predict a total of seven negative-parity states between 10.4 and 14.1 MeV, with a cross section at 14° of 1.5 mb/sr. Thus it appears that most of the $1\hbar\omega$ transition strength is predicted to lie at low excitation energies, as expected.

As will be discussed below, a multipole analysis of the data provides a minimum estimate of 6.9 mb/sr for the cross section at 14° for $\Delta L=1$ transitions to the region of excitation up to 20 MeV. This is more than 4 times the cross section predicted by the full shell model and 3 times the prediction for the total strength of the $1\hbar\omega$ excitations. It seems unlikely that such a large discrepancy could arise from uncertainties in the optical potentials assumed in the DWIA calculation given the good agreement for the ground-state transition. The use of a larger value of the oscillator parameter to simulate the spreading of the wave functions for unbound states resulted in a 40% decrease in calculated peak cross sections, as noted above. While this fails to account for the discrepancy, it does raise questions about the adequacy of the reaction model used to describe the excited-state transitions.

V. MULTIPOLE ANALYSIS

We have carried out a multipole analysis [21] of the data in order to search for GT and spin-dipole strength in the continuum above about 5 MeV excitation. In such an analysis, it is assumed that the angular distribution in each energy bin can be fitted with a sum of DWIA shapes for different values of the total angular momentum transfer and parity change ΔJ^π, so that

$$\sigma_{\text{expt}}=\sum_{\Delta J^\pi} a_{\Delta J}\sigma_{\text{DW}}(\Delta J^\pi) .$$

The coefficients $a_{\Delta J}$ are then obtained by carrying out a least-squares fit of this expression to the data.

In carrying out this analysis, it was first observed that for a given value of ΔJ^π, for the different transition amplitudes resulting from the shell model calculations, the DWIA shapes were generally characteristic of the value of ΔJ^π and similar to those predicted for simple proton-hole neutron-particle amplitudes. Consequently, it was assumed that the DWIA shapes required for the analysis could be calculated with the simple transition amplitudes shown in Table II. Calculations were carried out for excitation energies of 0, 10, 20, 30, and 40 MeV, with cross sections at other energies obtained by interpolation. The

TABLE II. Proton-hole neutron-particle configurations for DWIA calculation used in multipole analysis.

ΔJ^π	Proton hole	Neutron particle
1^+	$0s_{1/2}$	$0s_{1/2}$
0^-	$0s_{1/2}$	$0p_{1/2}$
1^-	$0s_{1/2}$	$0p_{3/2}$
2^+	$0s_{1/2}$	$0d_{5/2}$
3^-	$0s_{1/2}$	$0f_{7/2}$

shapes used in the analysis are shown in Fig. 6.

The qualitative behavior of the data in the region between 10 and 20 MeV excitation shows that transitions with $\Delta J^\pi = 1^-$ must be important. Furthermore, data at large angles and high excitation energies required contributions with $\Delta J > 1$. Since experimental results were available at only five angles, the number of calculated shapes used in the fitting was restricted to either 3 or 4. The following steps were followed in obtaining a final fit.

(i) $\Delta J^\pi = 1^+, 1^-, 2^+$. Using only these three DWIA shapes, the fit obtained at 2.7° is shown in Fig. 7. The importance of the $\Delta J^\pi = 1^-$ contribution is clearly seen. A small GT contribution is seen, with a cross section corresponding to a total strength $\sum B_{GT}(E_x) = 0.06$ unit. At 7.5° (not shown), the predicted cross section is consistently low in the region of 10 MeV excitation, and at 28° the fit at high excitation shows the need for contributions with $\Delta J > 2$.

It should be noted here that the model calculations predicted sizable cross sections for transitions to several

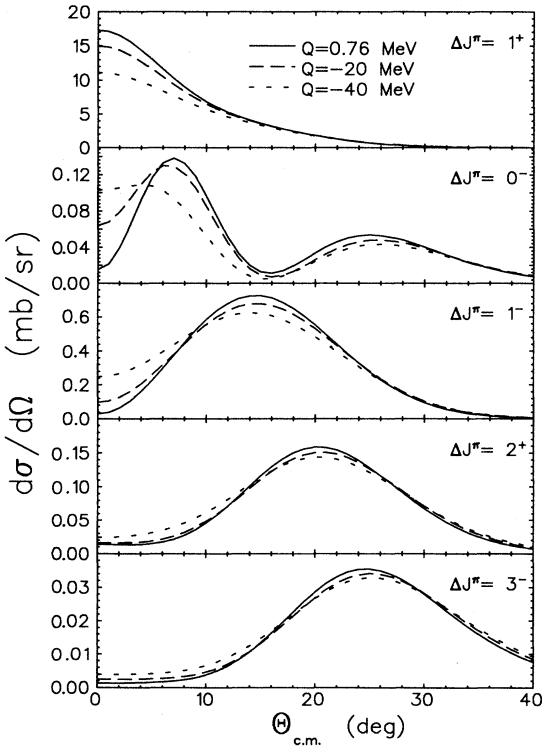

FIG. 6. DWIA shapes used in the multipole analysis. Calculations are shown for excitation energies from 0 to 40 MeV.

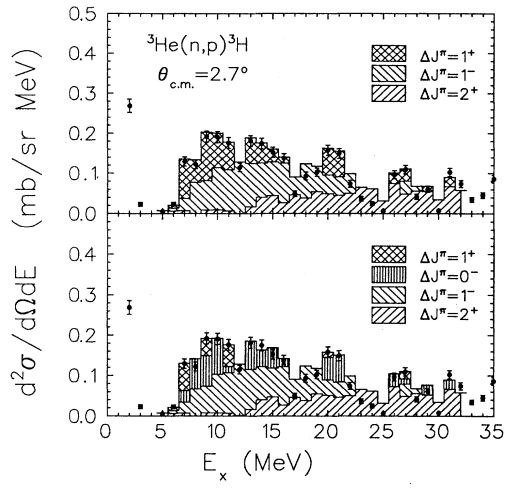

FIG. 7. Multipole analysis of data at 2.7° (c.m.) with three or four DWIA shapes allowed. Note that the $\Delta J^\pi = 1^+$ contribution in the upper panel is largely replaced by the 0^- contribution where this is allowed in the lower panel.

states with $\Delta J^\pi = 2^-$. The predicted shapes tended to peak at about 15°, as for $\Delta J^\pi = 1^-$ transitions, though they showed greater variability than the latter. It was assumed that the $\Delta J^\pi = 1^-$ component of the decomposition provided a reasonable estimate of the sum of $\Delta L = 1$ transitions for both 1^- and 2^- contributions.

(ii) $\Delta J^\pi = 1^+, 0^-, 1^- 2^+$. The shell model transition amplitudes predicted an appreciable cross section for transitions with $\Delta J^\pi = 0^-$ at low excitation energies. Such transitions proceed with $\Delta L = 1$, but the predicted angular distribution is characteristically different than those for $\Delta J^\pi = 1^-$ and 2^-, with a peak at 7.5° rather than 14°, as shown in Fig. 6. Consequently, the previous analysis was repeated with the addition of a contribution of this character, and the results are shown in Fig. 7 for an angle of 2.7°. Most of the cross section assigned as 1^+ in the first analysis is now represented by the 0^- contribution. The $\Delta J^\pi = 1^-$ contribution is unchanged. The fit is noticeably better at 7.5°, while the results at 28° still show the need for a contribution with $\Delta J > 2$.

(iii) $\Delta J^\pi = 1^+, 1^-, 2^+, 3^-$. Results for this case are shown in Fig. 8. As expected, the fits to the data at 2.7° and 7.5° are the same as in (i), while the fit at larger angles is improved by the addition of the contribution with $\Delta J^\pi = 3^-$. As in previous fits, the $\Delta J^\pi = 1^-$ contribution continues to dominate in the region of low excitation energy with a cross section at 14° of 7.6 mb/sr for transitions below 22 MeV excitation. This is to be compared with the DWIA prediction of 1.5 mb/sr at 14° for $\Delta L = 1$ transitions in this energy range.

(iv) $\Delta J^\pi = 0^-, 1^-, 2^+, 3^-$. Results for this case are shown in Fig. 9. The fits are almost as good as in (ii) at 1.7° and noticeably better at large angles. While the 0^- contribution has replaced the 1^+ contribution, the 1^- contribution is almost unchanged, with a 14° cross section of 6.9 mb/sr up to 22 MeV excitation. It should be noted that the 0^- component in the multipole analysis contributes a total of 1 mb/sr to the cross section between 7 and 16 MeV excitation at 7.5°, while DWIA cal-

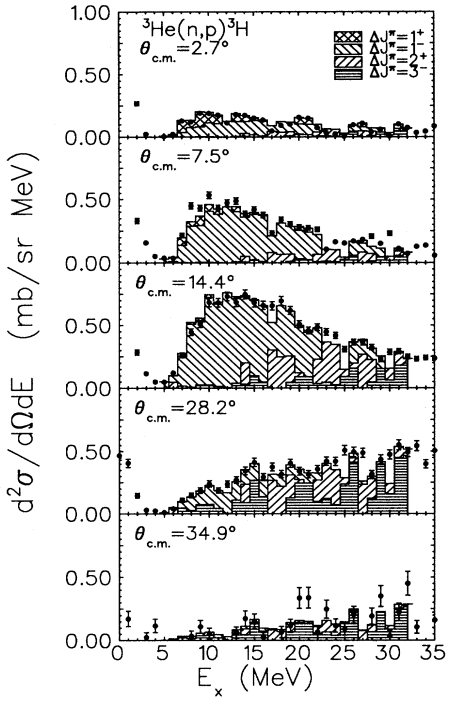

FIG. 8. Results of multipole analysis assuming a GT contribution to the cross section plus 1^-, 2^+, and 3^- contributions.

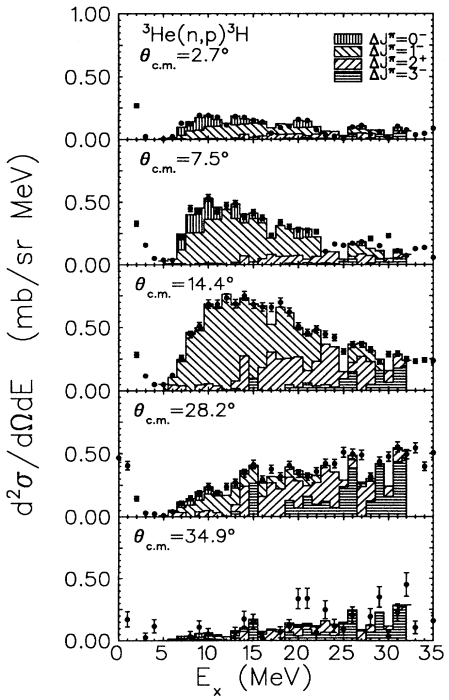

FIG. 9. Results of multipole analysis with the GT contribution of Fig. 9 replaced by a $\Delta J^\pi=0^-$ contribution. The overall quality of the fit is comparable with that shown in Fig. 8.

culations using the shell model transition amplitudes predict a total cross section at 7.5° of 0.13 mb/sr for transitions to three states at 10.04, 12.95, and 14.05 MeV. Thus the "measured" cross section from the multipole analysis is much greater than the DWIA prediction for 0^- transitions.

The results of analysis (i) show a $\Delta J^\pi=1^+$ (GT) contribution at excitation energies below 15 MeV with total strength of about one-quarter of the missing strength in the ground-state transition. The results of analysis (ii) show, however, that if a contribution with $\Delta J^\pi=0^-$ is allowed, then most of the "GT" strength in (i) is assigned as 0^-. The analyses in (iii) and (iv) simply show that the data can be adequately represented with the assumption of either a 1^+ or a 0^- contribution, along with 1^-, 2^+, and 3^- contributions of comparable magnitudes in each case. The final conclusion of this analysis of GT strength is that we are able to estimate an upper limit of about 0.06 unit for GT strength in the continuum concentrated in the region of 10 ± 4 MeV excitation. The identification of this strength is not certain, however, as the data can be fitted equally well with either $\Delta J^\pi=1^+$ or 0^- contributions in this region of excitation.

As noted above, the cross section for the $\Delta J^\pi=1^-$ contribution (which presumably includes contributions from transitions with $\Delta J^\pi=2^-$ also) is not much affected by the choice of 1^+ or 0^- in the analysis. In case (iii) with the $\Delta J^\pi=1^+$ shape, the 1^- contribution at 14° appears as a broad resonance between 6 and 22 MeV excitation. The integrated cross section at 14° is 7.6 mb/sr. In case (iv) with $\Delta J^\pi=0^-$, the distribution of 1^- cross sections is very similar to that in case (iii) with an integrated cross section at 14° of 6.8 mb/sr.

For transitions with $\Delta J^\pi=2^+$ and 3^-, analyses in cases (iii) and (iv) show similar strength distributions above an excitation energy of 22 MeV. At lower excitation energies, the analysis in case (iii) identifies the transition strength with $\Delta J^\pi=3^-$, with little 2^+ contribution. In case (iv) just the opposite is found with considerable $\Delta J^\pi=2^+$ strength and little $\Delta J^\pi=3^-$ strength. This result indicates that while the multipole analysis clearly requires contributions with $\Delta L>1$, the data are not complete enough to permit an unambiguous separation of different multipole contributions for $\Delta L>1$, at least at low excitation energies.

VI. SUMMARY AND CONCLUSIONS

This work was undertaken with two primary goals in view. The first of these was to determine the reduced cross section $\hat{\sigma}=\sigma(q=0)/B_{\rm GT}$ for $A=3$. The second was to search for GT strength in transitions to the continuum above the ground state.

The reduced cross section was found to have the value $\hat{\sigma}=6.9\pm0.2$ in units such that the GT sum rule has a value $3(N-Z)$. It is interesting to note that this value of $\hat{\sigma}$ for $A=3$ is substantially less than the value $\hat{\sigma}\simeq10$ measured [22] for nuclei in the mass range $6\leq A\leq13$ for incident energy of 200 MeV. Although the energy is higher in this measurement, studies [23,24] of the ^{7}Li(p,n) reaction at energies of 200 MeV and above show little

dependence of cross sections on incident energy, so that a comparison of the present result with those at 200 MeV should be significant.

The search for GT strength in excited-state transitions was carried out through a multipole analysis of the available data at five angles. This analysis showed that the data are consistent with a small amount of GT strength in the region of excitation between 7 and 16 MeV. From the measured value of σ, the magnitude of possible GT strength was established as $\sum B_{\mathrm{GT}}(E_x)=0.06$ units or about one-quarter of the strength missing in the ground-state transition. It was found, however, that the data could be equally well fitted by a multipole analysis in which the GT contribution was replaced by a contribution from transitions with $\Delta J^{\pi}=0^{-}$. Thus the results are consistent with no GT strength in the continuum and with an upper limit of about one-quarter of the missing strength predicted by the GT sum rule.

A third result from these measurements is the identification of a broad resonance in the cross section between 10 and 20 MeV excitation for transitions with $\Delta J^{\pi}=1^{-}$. This presumably arises from the expected spin-dipole giant resonance associated with transitions from the 0*s* to 0*p* shell model orbits. It was found, however, that DWIA calculations using transition amplitudes from large-scale shell model calculations did not agree with measured cross sections above the ground state. The cause of the discrepancy is not known, though there is some reason to question the reaction model for excited-state transitions.

ACKNOWLEDGMENTS

We wish to thank Dr. P. W. Green for his assistance with the data acquisition system used in these measurements. B. Larson, J. Mildenberger, S. Ram, and A. Yavin also assisted in carrying out the measurements. This work was supported by grants from the National Research Council and from the Natural Sciences and Engineering Research Council of Canada, and by NSF Grant No. PHY-90-17077.

[1] G. F. Bertsch and I. Hamamoto, Phys. Rev. C **26**, 1323 (1982).
[2] I. S. Towner and F. Khanna, Nucl. Phys. **A399**, 334 (1983).
[3] J. J. Simpson, Phys. Rev. C **35**, 752 (1987).
[4] T.-Y. Saito, Y. Wu, S. Ishikawa, and T. Sasakawa, Phys. Lett. B **242**, 12 (1990).
[5] T. N. Taddeucci *et al.*, Nucl. Phys. **A469**, 125 (1987).
[6] R. Helmer, Can. J. Phys. **65**, 588 (1987).
[7] R. S. Henderson *et al.*, Nucl. Instrum. Methods A **286**, 41 (1991).
[8] B. W. Pointon *et al.*, Phys. Rev. C **44**, 2430 (1991).
[9] A. Celler *et al.*, Phys. Rev. C **43**, 639 (1991).
[10] R. A. Arndt and L. D. Roper (unpublished); R. A. Arndt *et al.*, Phys. Rev. D **45**, 3995 (1992).
[11] R. Caeuleneer, P. Vanderputte, and C. Semay, Phys. Lett. B **196**, 303 (1987).
[12] T. Sasakawa and S. Ishikawa, Few Body Syst. **1**, 3 (1986).
[13] B. A. Brown, A. Etchegoyen, W. D. M. Rae, and N. S. Godwin, MSUCL Report No. 524, 1986.
[14] A. Hosaka, K. I. Kubo, and H. Toki, Nucl. Phys. **A444**, 76 (1985).
[15] W. G. Love, in *The (p,n) Reaction and the Nucleon-Nucleon Force,* edited by C. D. Goodman *et al.* (Plenum, New York, 1980), p. 23.
[16] G. Retzlaff and D. M. Skopik, Phys. Rev. C **29**, 1194 (1984).
[17] R. Schaeffer and J. Raynal, computer code DWBA70 (unpublished); J. R. Comfort, computer code DW81 (extended version of DWBA70), Arizona State University, 1984.
[18] W. T. H. van Oers *et al.*, Phys. Rev. C **25**, 390 (1982).
[19] W. R. Gibbs and B. F. Gibson, Phys. Rev. C **43**, 1012 (1991).
[20] M. A. Franey and W. G. Love, Phys. Rev. C **31**, 488 (1985).
[21] M. A. Moinester, Can. J. Phys. **65**, 660 (1987).
[22] K. P. Jackson *et al.*, Phys. Lett. B **201**, 25 (1988).
[23] J. W. Watson *et al.*, Phys. Rev. C **40**, 22 (1989).
[24] T. N. Taddeucci *et al.*, Phys. Rev. C **41**, 2548 (1990).